ISSN: 2688-8653

Metabolomic and Network Pharmacology Studies on the Anti-Atherosclerotic Mechanism of Melatonin and Multi-Omics Studies on the Atherosclerosis Mechanism

Hao Xue[1], Siyu Zhao[1], Xiangxue Wang[1], Naijun Hu[1], Wenhan Liu[1], Feng Xu[2], Jianzhong Bi[1], Chao Lai[1] and Zhaohong Xie[1,*]

[1]School of The Second Hospital, Cheeloo College of Medicine, Shandong University, Jinan 250033, China;

[2]School of Management, Shandong University, No. 27, Shanda South Road, Jinan, 250100, China.

[*] Corresponding Author: xie_zhaohong@sdu.edu.cn.

Abstract

Atherosclerosis (AS) has become the leading reason of ischemic heart disease and many other diseases. Current discoveries give only a brief glimpse of the mechanisms involved. Melatonin is beneficial in the treatment of AS. However, further studies are required to identify the possible mechanisms. This study aimed to evaluate the underlying pathological mechanisms involved in AS and the mechanisms of melatonin's effect against AS. Furthermore, this study evaluated the biological functions of the metabolome and proteome of iliac artery samples in different AS stages and healthy controls. Then, investigating the key mechanisms of melatonin against different stages of AS by metabolomics and network pharmacology. Purine nucleotides metabolism was found to be related to atherosclerotic plaque without lipid core stage and purine metabolism was found to be related to subclinical atherosclerotic stage and atherosclerotic plaque with lipid core stage, indicating purine nucleotide metabolism may be disrupted in arterial intima thickening stage and has been disrupted in atherosclerotic plaque without lipid core stage. We found many amino acids, such as alanine, aspartate, glutamate, and arginine, were associated with different stages of atherosclerosis. After identifying three hub targets (NOS3, PLA2G10, and MPO), additional molecular docking studies revealed a strong affinity between melatonin and significant targets. The current study emphasized the key roles of purine and purine nucleotide metabolism in the development of AS and showed the clinical characteristics and potential treatment targets implicated in various stages of AS. Moreover, further study revealed the therapeutic mechanisms of melatonin in different stages of AS. This study showed a novel concept for identifying potential pharmacological mechanisms.

Keywords

Atherosclerosis, Multiomics, Melatonin, Network pharmacology, Mechanisms.

1. Introduction

Atherosclerosis (AS) is a chronic inflammatory condition of the arteries and is associated with a 50% mortality rate in developed countries. It is mostly a lipid-driven process that is triggered by an active inflammatory process, a buildup of low-density lipoprotein and residual lipoprotein particles, and focal regions of arteries. Large and moderate-sized arteries likely develop considerable stenosis from the long-term accumulation of vessel-occluding plaques in the subendothelial intimal layer, which reduces blood flow and leads to critical tissue hypoxia.

ISSN: 2688-8653

Myocardial infarction and stroke are the most common causes of death around the world. They are both caused by spontaneous thrombotic vascular occlusion [1]. The bulk of atherogenesis research focuses on the creation and architecture of vascular plaques [2]. Current papers have discovered that subclinical atherosclerosis is an important predictor of atherosclerotic load and that reversing it may help avoid the development of clinical cardiovascular disease [3]. However, the discoveries are hard to convert into preventative indicators for regular diagnostics and give only a brief glimpse of the mechanisms involved. Consequently, identifying new biochemical indicators would be very beneficial not only to gain a deeper knowledge of the underlying mechanisms but also to enhance earlier diagnosis, monitoring, and treatment of AS. As scientific knowledge grows and technology progresses, several biomarkers based on the size of individual molecules will be found, analyzed, and studied. A few such compounds have been suggested in AS, including microRNA-217 [4], and several are in the process of being validated for usage in research and clinical contexts [5]; nonetheless, potential metabolites for detecting AS patients need to be further investigated and optimized. Weighted gene coexpression network analysis (WGCNA) is a topological approach that has been shown to find new mechanisms and therapeutic targets in multi-omics investigations. WGCNA could also help figure out if there is a link between omics data and clinical phenotypes [6].

Both the innate and adaptive immune systems play critical roles in the development and progression of AS, which is a chronic inflammatory process. Plaque formation can be suppressed. Additionally, in some cases, the disease can even regress when these particular pathways are targeted, as shown in experimental models. As a result, it is reasonable to anticipate the development of anti-inflammatory treatments [7]. Melatonin (N-acetyl-5-methoxytryptamine) is primarily generated by vertebrates' pineal glands as a hormone. Since mitochondria where free oxygen radicals are generated produce melatonin, melatonin is recognized as a potent free oxygen radicals scavenger [8]. Melatonin is well recognized for its anti-inflammatory and immune-regulating effects, and numerous studies have shown melatonin is involved in and affects several pathophysiological processes such as angiogenesis [9], pyroptosis [10], metabolic abnormalities of glucose and lipids [11,12], apoptosis [13], and autophagy [14]. Apart from its principal usage in the treatment of sleep problems, melatonin also possesses vascular-protective qualities [15-17]. According to reports, melatonin has many preventive properties against cardiovascular disease by avoiding pyroptosis in the endothelium [18], exhibiting antioxidant capacity [19], and restricting neutrophil migration [20]. Owing to the possible advantages in the treatment of AS and its good level of safety [21, 22], melatonin may be used as an adjuvant in people with AS. However, the therapeutic mechanisms and targets of Melatonin against AS remain elusive. An effective method based on network pharmacology and metabolomics has already been shown in elucidating therapeutic targets and processes [23].

In this view, WGCNA was used for proteomic and metabolomic assay to elucidate the new molecular hallmark of AS and subclinical atherosclerosis. For the objective of this research, subclinical atherosclerosis is the term used to describe the early intimal thickening that occurs before lipid buildup and the creation of early plaques [24]. Subsequently, the pathways correlated with the biomarkers mentioned were investigated to identify potential therapeutic or preventative targets. Herein, the metabolomics analysis was further integrated with network pharmacology and analyze the reactions that regulate the metabolites and the targets that melatonin acted on in different stages of AS. This approach may help to comprehend the therapeutic mechanisms of melatonin for the management of AS.

Herein, a new method was initially developed to explore the primary targets and the AS therapeutic mechanisms at various stages before elucidating the new mechanisms of AS progression. This study showed how melatonin can be used as a treatment for AS at different stages.

ISSN: 2688-8653

2. Materials and Methods

2.1. Subjects

From August 2020 to December 2021, a total of 19 iliac artery samples from 8 patients with atherosclerosis (AS) (AS group or AS with/without lipid nucleus group), 3 patients with subclinical atherosclerosis (Arterial intima thickening group), and 6 health control individuals without AS (HC group) were enrolled in this research (Figure 1), and these samples were taken at the Second Hospital of Shandong University (Shandong, China). The approval of procedures used in this study was provided by the Clinical Research Ethics Committee of the Second Hospital, Shandong University, China. Furthermore, the informed consent form was signed by the participant or their legal representatives. Herein, the presence of AS was recorded which indicated a positive result on artery ultrasound (any plaque with/without lipid nucleus), subclinical atherosclerosis which we defined as a positive result on artery ultrasound (intimal thickening without any plaque), and HC, which we defined as a negative result on artery ultrasound [25]. Before further assessment, all arterial samples were immediately frozen using liquid nitrogen and maintained at −80°C.

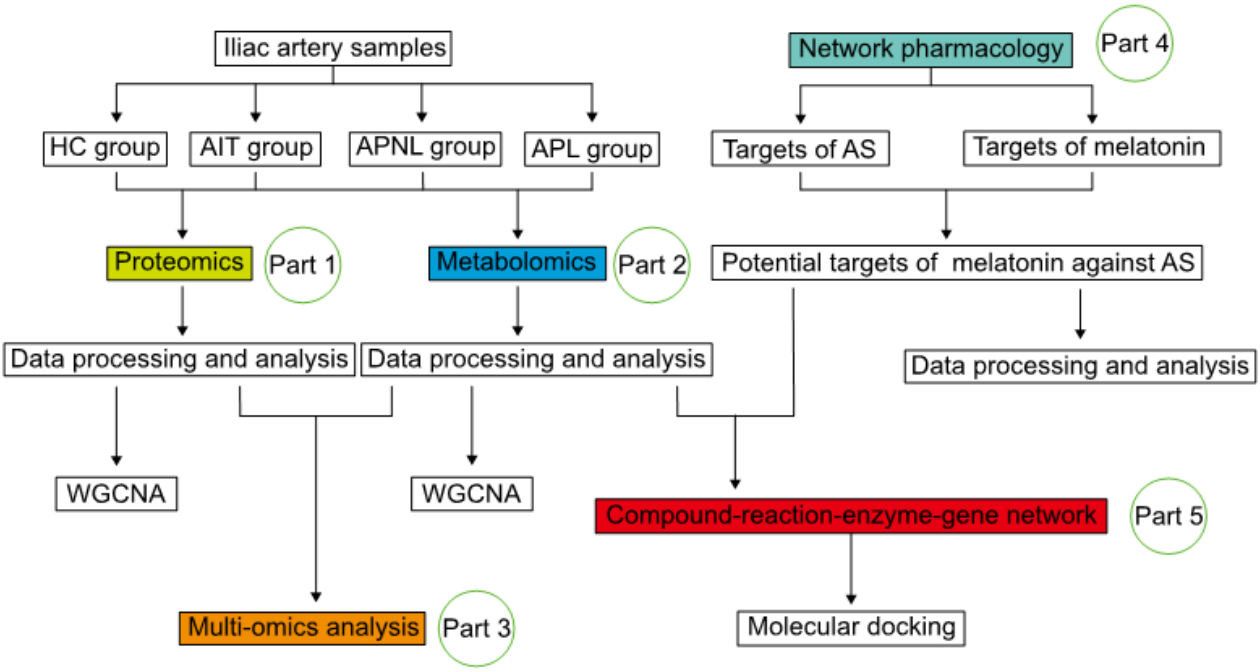

Figure 1: The schematic flowchart of the integrated strategy. The mechanisms of AS progression were analyzed by proteomics, metabolomics, and multi-omics (Part 1, Part 2, and Part 3). Potential targets were extracted by network pharmacology (Part 4). The compound-reaction-enzyme-gene networks were constructed. Key targets were further verified by molecular docking (Part 5).

2.2. Proteomic LC-MS/MS analysis

UA buffer, which had 150 mM Tris-HCl at pH 8.0 and 8 M Urea, was used to eliminate the detergent and other low-molecular-weight (10 kD) substances. In order to prevent decreased cysteine residues, 100 μl of iodoacetamide (100 mM IAA in UA buffer) was then added. Next, the samples were incubated in the absence of light for 30 minutes. According to the process of Matthias Mann's filter-aided sample preparation (FASP), trypsin was used for protein digestion. Based on how much tyrosine and tryptophan are in proteins from vertebrates, a 0.1% (g/l) solution with an extinction coefficient of 1.1 was used to measure the composition of peptides

ISSN: 2688-8653

using the UV light spectral density at 280 nm. The LC-MS/MS study was performed by connecting a Bruker TimsTOF Pro-mass spectrometer to a Bruker Daltonics Nanoelute for high-resolution mass spectrometric mapping. In order to isolate the peptides, a linear gradient of buffer B (containing formic acid and acetonitrile with 0.1% and 84% compositions, respectively) was applied at a flow rate of 300 nl/min using IntelliFlow, and the reverse phase trap column (Thermo Scientific Acclaim PepMap100, 100 μm×2 cm, nanoViper C18) was linked to the C18 reversed-phase analytical column. Positive ion mode was used to operate the MS. Following 10 cycles of PASEF MS/MS with a baseline intensity of 1.5K and a threshold of 2500, the MS obtained ion mobility MS spectra throughout a mass range of m/z 100–1700 and 1/k0 of 0.6 to 1.6. A relaxation time of 0.4 minutes allowed for the activation of active exclusion.

2.3. Online database searching and protein analyses

Using the MaxQuant search engine, the LC-MS/MS spectral data were compared to proteins from Homo sapiens in the SwissProt database (version 1.5.3.17). The tolerance for the mass of the fragment ion and the precursor mass were both set to 20 ppm. Carbamidomethyl was considered a fixed variation, while methionine oxidation was designated as a dynamic variation. For trypsin, it was acceptable to miss two cleavages. In order to filter the outcomes, a false discovery rate of 1% was applied at both the peptide and protein levels. Furthermore, proteins were quantified by using a razor and certain peptides. It was necessary to have a peptide ratio count of at least one. As a result, a total of 3723 proteins were found in the arterial samples.

2.4. LC MS-based metabolomics analysis

In the current study, a Vanquish ultra-high-pressure liquid chromatography (UHPLC) with Q-Exactive HF-X mass (Thermo Scientific, Shanghai, China) was used to perform the metabolomics analysis. The samples were evaluated by a 2.1 mm × 100 mm ACQUIY UPLC BEH Amide 1.7 m column for hydrophilic interaction liquid chromatography (HILIC) separation (waters, Ireland). A = 25 mM ammonium acetate and 25 mM ammonium hydroxide in water were present in the mobile phase of electrospray ionization (ESI) in both positive and negative ion modes, and B = acetonitrile. The gradient was 98% B for 1.5 minutes, linearly decreased to 2% in 10.5 minutes, maintained for 2 minutes, increased to 98% in 0.1 minutes, and then stabilized for 3 minutes. The following parameters were used to generate ESI: Source temperature: 600 °C, IonSpray Voltage Floating (ISVF) 5500 V, Ion Source Gas1 (Gas1) as 60, Ion Source Gas2 (Gas2) as 60, curtain gas (CUR) as 30. After configuring the instrument for MS-only acquisition with an m/z range of 80–1200 Da, a resolution of 60000, and an accumulation period of 100 ms, we were able to successfully acquire a sample. An automatic MS/MS acquisition was used with the following parameters set: resolution, 30,000; m/z range, 70–1200 Da; accumulation time, 50 ms; exclude time, 4 sec.

2.5. Analyzing metabolomic data

Proteo Wizard MS Convert was used to convert the raw MS data into MzXML files, which were then imported into the free XCMS software. The following parameters were used for peak picking: peakwidth = c (10, 60), prefilter = c, and centWave m/z = 10 ppm (10, 100). For the grouping of peaks BW = 5, mZwid = 0.025, and minfrac = 0.5 were used. In the current study, CAMERA was employed for annotating isotopes and adducts. The retrieved ion characteristics were filtered to keep only the variables with more than 50% of the non-zero data values in at least one group. By the comparison of m/z values (<10 ppm) and MS/MS spectral data with private datasets built using freely available authentic standards, compound identification of metabolites was carried out [6,26]. The detected metabolites met or exceeded all criteria established by the Metabolomics Standards Initiative's Chemical Analysis Working Group for levels 2 or higher. To identify metabolic pathways, the KEGG pathway database and metabolomic data interpretation were performed by Metabo Analyst.

ISSN: 2688-8653

2.6. Protein/Metabolite coexpression network analysis

Using network analysis, modules of coexpressed proteins/metabolites were identified. To establish protein/metabolite coexpression networks, the WGCNA R package was used to normalize protein/metabolite abundance. Following parameters were sent to the WGCNA:blockwiseModules() function: soft threshold power β = 8 for proteins/ 9 for metabolites, minModuleSize = 30, mergeCutHeight = 0.15 for proteins/ 0.25 for metabolites and default values were applied to all other parameters. Soft threshold power β specified strong protein/metabolite connections and penalized weak correlations. By clustering strongly associated proteins/metabolites into modules, the dimensions of the dataset were decreased. KME was defined as the module membership measure. The association between module and sample clinical features was deduced to ascertain protein/metabolite modules that were closely related to the key clinical phenotypes. Proteins that serve as hubs in modules with important therapeutic implications were identified as potential proteins that are essential for disease pathophysiological evaluation. Herein, hub proteins were characterized by affiliated value >0.8 and a link with clinical traits >0.6. Functional enrichment analyses were carried out using the Cluster Profiler package of R 4.1.3. [27]. MetaboAnalyst platform conducted functional annotation analysis for metabolites.

2.7. Multiomics data integration

To combine the analysis of metabolomics and proteomic data, CCA (sparse canonical correlation analysis) was performed using the DIABLO [28] in the Mix-Omics program [29]. The generalized, automated partial least-squares method was employed to combine different types of data for similar biological samples and to find important omics features across multiple datasets at the same time.

2.8. Identification of potential melatonin targets

Pub Chem (https://pubchem.ncbi.nlm.nih.gov/) database was used to obtain the 3D structure of melatonin and its SMILES (simplified molecular input line entry specification) [30]. To identify potential melatonin targets, the 3D structure of melatonin was uploaded to the PharmMapper Server (http://www.lilab-ecust.cn/pharmmapper/), and its SMILES were uploaded to the TargetNet database (http://targetnet.scbdd.com/home/index/) and SwissTargetPrediction databases (http://targetnet.scbdd.com/home/index/) [31-33]. DrugBank (https://go.drugbank.com/) and TCMSP (https://tcmspw.com/tcmsp.php) databases were utilized to find recognized targets of melatonin [34,35]. Furthermore, Uni Prot (https://www.uniprot.org) was employed to change the names into official symbols.

2.9. Assortment of AS-linked targets

The databases, including Gene-Cards (https://www.genecards.org), DisGeNET (https://www.disgenet.org), and NCBI Gene (https://www.ncbi.nlm.nih.gov/gene/) were used to find targets associated to AS. The keyword here was atherosclerosis. DisGeNET's AS-linked targets with a gene-disease score of ≥ 0.1 and GeneCards' relevance score criterion of 10 were both set to boost the veracity of the findings.

2.10. Evaluation of Protein-Protein Interaction (PPI)

The STRING (https://string-db.org) platform was utilized to extract information on protein-protein interactions [36]. The score of interaction confidence was set to 0.7, which on the STRING platform denotes high confidence, and the species was confined to "Homo sapiens."

2.11. Enrichment of common genes in GO and KEGG pathways

Using the R-version 4.1.3 clusterProfiler, gene ontology (GO) and KEGG pathway enrichment analysis was carried out on the shared genes for melatonin and AS to elucidate the key function

ISSN: 2688-8653

of therapeutic targets in gene function and signaling cascade [27]. The route class of each KEGG pathway was taken from the KEGG for additional analysis.

2.12. Network construction of network pharmacology

Five networks were created: (1) Melatonin and its targets were connected to form the melatonin-potential target network; (2) AS targets in the PPI network; (3) a second PPI network was built utilizing melatonin and AS genes that intersected; (4) Melatonin, its targets, and important pathways were linked to form the melatonin-targets-pathways network. Using the Community Cluster method (Glay) of clustermaker2, the network was separated into functional modules for further analysis [37]; (5) Sub-networks of possible therapeutic targets were constructed that were enriched in specific types of major pathway classes. Using Cytoscape 3.9.1, each of the aforementioned networks was created.

2.13. Target protein preparation

The RCSB Protein Data Bank (http://www.rcsb.org) was employed to find the protein receptor crystal structures. The original ligand, solvent molecules, superfluous protein chains, and hydrogen atoms were removed from the retrieved protein structures using PyMol 2.5.3. The Gasteiger was then calculated, together with the center and size of the docking box, using AutoDock Tools 1.5.7. [38].

2.14. Molecular docking

The analysis of the hub targets and melatonin interaction was then carried out using molecular docking with AutoDock Vina [39]. AutoDock Tools version-1.5.7 was employed to convert the structures of each protein and melatonin to the PDBQT format necessary for molecular docking. With the help of AutoDock Vina, melatonin was attached to the proteins. Afterward, the AutoDock Vina computed interactions were tallied, and the PyMol 2.5.3 program was used to show the docking result.

2.15. Statistical analysis

The R limma's (normalize between arrays) function was used to normalize the protein and metabolite abundance. Unless otherwise stated, statistical analysis was carried out using R software. The implication of differences between two sets of independent variables was assessed using the Student's t-test. Orthogonal partial least-squares discriminant analysis (OPLS-DA) was performed by R package (ropls). Log2 fold change (FC)>2.0, P-value<0.05 was used to define differentially expressed proteins (DEPs), and variable importance in the projection (VIP)>1.0, P-value <0. 05 were used to define differentially expressed metabolites (DEMs). Analyses of functional enrichment were conducted on changed proteins and co-expressed modules that were strongly linked with illness state by using R-version 4.1.3 clusterProfiler [27]. The significance of functional enrichment analysis was determined by P-value <0.05. MetaboAnalyst platform (http://www.metaboanalyst.ca/MetaboAnalyst/) conducted functional annotation analysis for metabolites.

3. Results

3.1. Proteomic characteristics of patients with different stages of AS

3723 proteins were identified in total. To explore if individuals with different stages of AS had diverse protein expression patterns, differential expression analysis of proteomic profiles was conducted using a P-value <0.05 and a difference in expression levels ≥ 2.0-fold.

There were 96 differential proteins between arterial intima thickening (AIT) and HC groups, with 71 down-regulated and 25 up-regulated. A total of 97 differential proteins were determined between atherosclerotic plaque without lipid core (APNL) and AIT groups, with 35

ISSN: 2688-8653

down-regulated and 62 up-regulated. With 13 up-regulated and 25 down-regulated proteins, there were 38 different proteins between the atherosclerotic plaque with lipid core (APL) and APNL groups. 123 differential proteins were determined between atherosclerotic plaque (AP) and AIT groups in total, with 49 up-regulated and 74 down-regulated (Supplementary Figure 2; Supplementary Tables 1-4). Hierarchical cluster analysis plots based on DEPs showed a clear separation between each stage of AS (Supplementary Figure 1). Significantly altered gene ontology (GO) terms such as phosphatidylcholine binding, fatty-acyl-CoA binding, receptor catabolic process, blood microparticle, and high-density lipoprotein particle clearance were strongly enriched with DEPs between AIT and HC groups. Between the APNL and AIT groups, DEPs were highly enriched for the significantly altered gene ontology (GO) terms positive regulation of type-I interferon (IFN)-regulated signaling cascade, cytosolic large ribosomal subunit, an intrinsic component of mitochondrial membrane, and ubiquitin protein ligase binding. The GO terms glycosaminoglycan binding and extracellular matrix organization were highly enriched with DEPs between APL and APNL groups. The significantly altered gene ontology (GO) terms negative regulation of intrinsic apoptotic signaling pathway, oxidoreductase complex, proteasome complex, inner mitochondrial membrane protein complex, and endopeptidase complex were highly enriched with DEPs between AP and AIT groups (Supplementary Figure 3; Supplementary Tables 5-8).

3.2. Construction of a protein co-expression network

Pairwise relationships among proteins obtained from a matrix of protein expression values were used to form a network of protein co-expression using WGCNA. There are 22 protein high co-expression modules in all, and they are shown in different colors (Figure 2A). These modules share comparable expression patterns across the cases under study. These modules varied in size from 491 proteins to 38 proteins. To determine the relevance between each module and the illness condition, two methodologies were used (Figure 2B). It was believed that a stronger correlation between modules and illness state corresponded to higher module significance. The correlation between module participation and disease phenotypes was also calculated. The result indicated that the tan module was highly correlated with AIT, the light-yellow module was found to be considerably related to APNL, and the pink module was highly correlated with APL and AP. Both the eigenprotein value of the module tan and the module light-yellow significantly increased in the AIT (Figure 3A) and APNL (Figure 3C) phenotypes, respectively. Across the APL and AP phenotypes, the eigenprotein value of module pink considerably dropped (Figure 3E). Functional enrichment study revealed that the multivesicular body, ligase activity, Gβγ (G-protein beta-gamma) dimeric protein complex binding, generating carbon-sulfur bonds, and sodium:potassium-exchanging ATPase complex were all enriched in the proteins of module Tan (Figure 3B; Supplementary Table 9). These results demonstrated that regulation of the vesicle lumen (e.g., extracellular matrix), inflammation, lipid metabolism, and oxidative stress might be central to the pathophysiology of AIT. Functional enrichment analysis indicated that the proteins of module light-yellow were enriched in purine ribonucleoside triphosphate biosynthetic process, extracellular matrix structural constituent conferring tensile strength, cytosolic large ribosomal subunit, and inner mitochondrial membrane protein complex (Figure 3D; Supplementary Table 10). According to these results, regulation of purine nucleotide, extracellular matrix, ribosome, and mitochondria might be central to the pathophysiology of APNL. Functional enrichment analysis indicated that the proteins of module pink were enriched in regulation of Arp2/3 complex-mediated actin nucleation, clathrin adaptor complex, cytosolic large ribosomal subunit, cellular response to insulin stimulus, and inner mitochondrial membrane protein complex (Figure 3F; Supplementary Table 11). Moreover, this data demonstrated that regulation of actin, ribosome, clathrin, insulin, and mitochondria might be central to the pathophysiology of APL and AP.

ISSN: 2688-8653

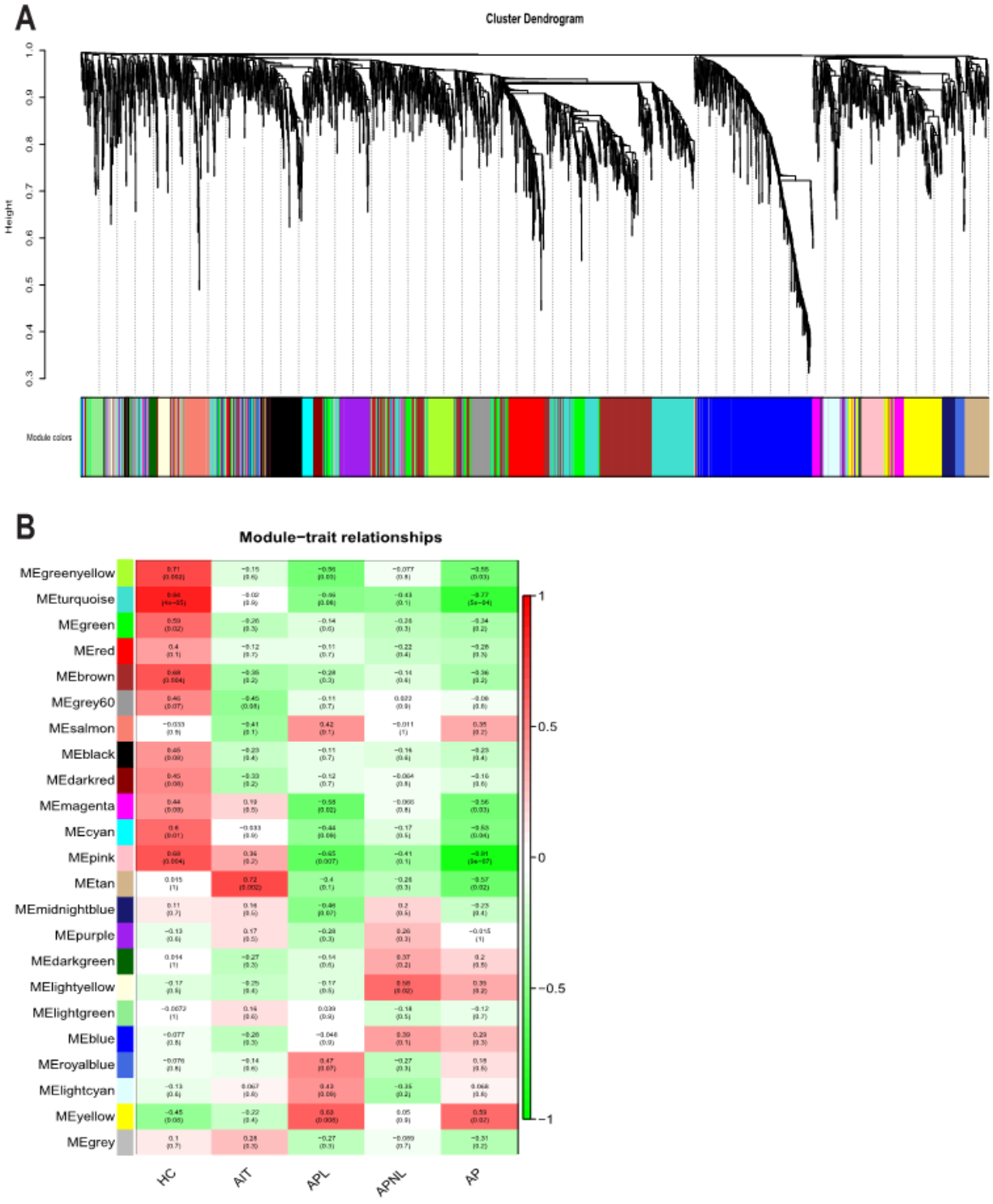

Figure 2: (A) Cluster dendrogram and distinct protein co-expression modules defined by dendrogram branch cutting of all proteins. (B) Heat map representation of Pearson's correlation between module eigenproteins and different phenotypes.

ISSN: 2688-8653

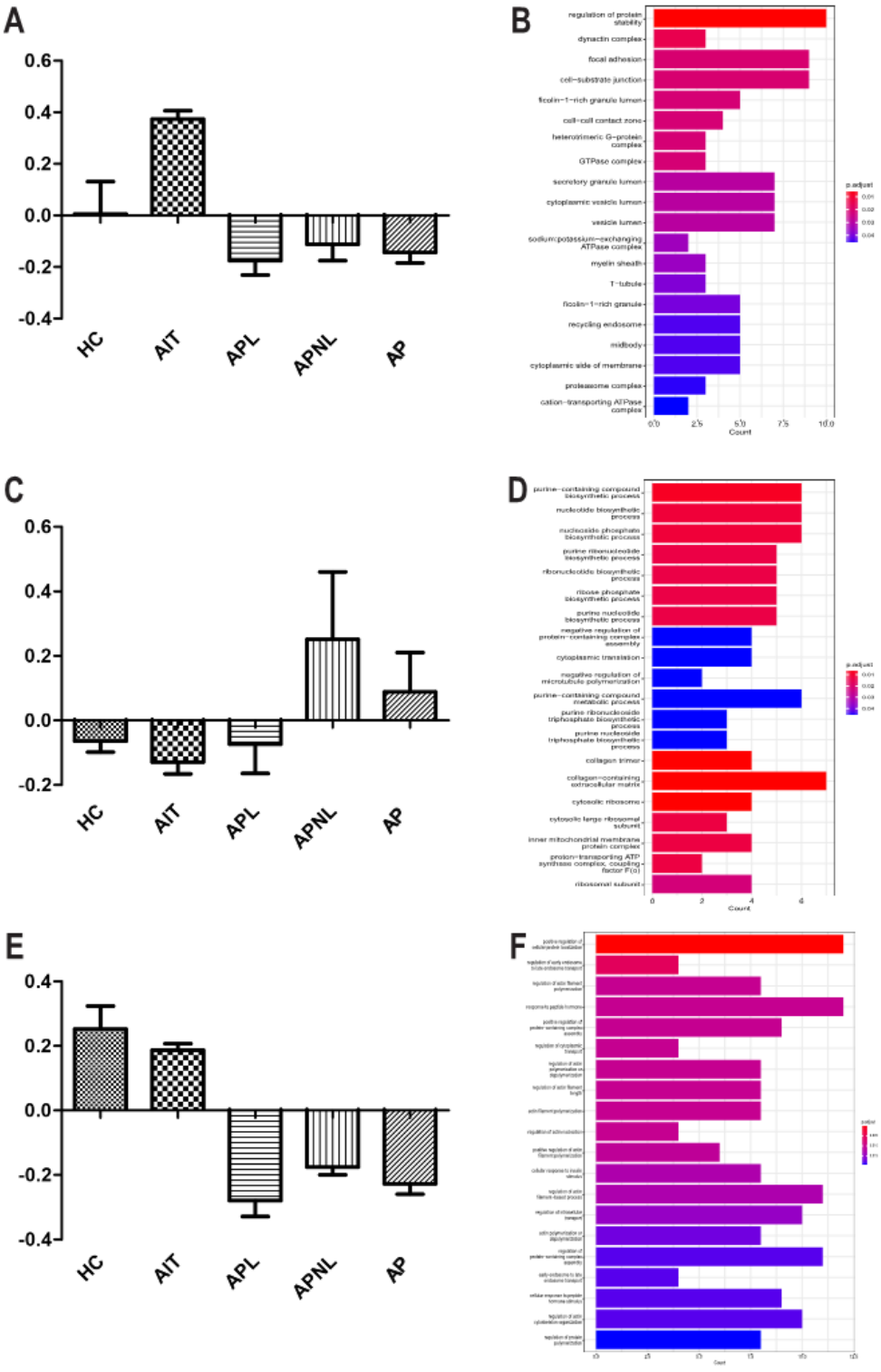

Figure 3: (A) Synthetic eigenprotein analysis for the tan module, which is highly correlated with AIT patients. (B) Gene Ontology terms enriched in the tan module. (C) Synthetic eigenprotein analysis for the light-yellow module, which is highly correlated with APNL patients. (D) Gene Ontology terms enriched in the light-yellow module. (E) Synthetic eigenprotein analysis for the pink module, which is highly correlated with APL and AP patients. (F) Gene Ontology terms enriched in the pink module.

ISSN: 2688-8653

3.3. Identification of key proteins

97 proteins were associated with the tan module. 49 proteins were associated with the light-yellow module. There were 128 protein connections to the pink module. Scatterplots showed a high association of these proteins in each module. A weighted sub-network of each module's proteins was created to better investigate the key proteins in each module. Four proteins were found to be hub proteins of the light-yellow network, 28 proteins were found to be hub proteins of the pink network for APL, and 74 proteins were found to be hub proteins of the pink network for AP. The tan network hub proteins were identified as 14 proteins, the light-yellow network hub proteins as 4, and the pink network hub proteins as 28 proteins. These proteins were specifically expressed in various stages of AS (Supplementary Figure 4).

3.4. Analysis of unspecified metabolomic profiles from AS patients at varying stages

Quality control (QC) sample chromatograms revealed that the retention times and response intensities of chromatographic peaks substantially overlapped, indicating instrument stability, which is essential for the collection of accurate nonspecific metabolomic data. Among the 2,439 metabolites observed were organic acids and their derivatives, organic oxygen compounds, lipids, and lipid-like substances, organoheterocyclic compounds, benzenoids, etc (Supplementary Figure 6). To explore if individuals with diverse phases of AS had varied patterns of metabolite expression, differential expression analysis of metabolomic profiles was performed using a P-value <0.05 and OPLS-DA VIP>1 (Supplementary Figure 5; Supplementary Tables 12-15). Hierarchical cluster analysis plots based on DEMs showed an obvious separation between each stage of AS (Supplementary Figure 7). There were significant differences in the levels of 31 metabolites between the AIT and HC groups and 24 metabolites between the APNL and AIT groups, 52 metabolites between the APL and APNL groups, and 17 metabolites between the AP and AIT groups in positive ion mode and negative ion mode, respectively. Metabolite pathway analysis showed that DEMs between AIT and HC groups were most enriched in the synthesis and degradation of ketone bodies, ascorbate and aldarate metabolism, purine metabolism, and butanoate metabolism. The analysis of metabolite pathways revealed that DEMs between APNL and AIT groups were enriched in nicotinate and nicotinamide metabolism. Furthermore, metabolite pathway analysis also indicated that DEMs between APL and APNL groups were enriched in the metabolism of amino acids, such as methionine and cysteine metabolism, biosynthesis of phenylalanine, tyrosine, and tryptophan, metabolism of arginine and proline, and glycine, serine and threonine metabolism, etc. Moreover, the analyses of these metabolite pathways indicated that DEMs between AP and AIT groups were most enriched in purine metabolism and pentose phosphate pathway (Supplementary Figure 6; Supplementary Tables 16-19).

3.5. Construction of a metabolite co-expression network

Using WGCNA, a metabolite co-expression network was created. In total, 16 metabolite modules with high co-expression were identified. The size of the modules varied between 44 and 338 metabolites (Supplementary Figure 8). A correlation analysis was done between each metabolite module and the illness phenotype to determine whether modules were substantially connected with the clinical phenotypes of interest. Based on these results, module purple has a strong relationship with AIT (R = 0.57, P value = 0.02). The results demonstrated that module pink has a strong relationship with APNL (R = 0.38, P value = 0.1). The results demonstrated that module blue has a strong relationship with APL (R = 0.58, P value = 0.02). The results demonstrated that module light-cyan has a strong relationship with AP (R = −0.49, P value = 0.05) (Figure 4A). The eigenmetabolite value of module purple was found to be considerably elevated in the AIT phenotype, the eigenmetabolite value of module pink rose considerably in

ISSN: 2688-8653

the APNL phenotype and the eigenmetabolite value of module blue rose considerably in the APL phenotype (Figure 4C-E). Similarly, the module light-cyan eigenmetabolite value fell considerably in the AP phenotype (Figure 4F). Lipids and lipid-like substances, Organic acids and their derivatives, benzenoids, and organoheterocyclic compounds were the vast majority of the metabolite of the purple, pink, blue and light-cyan modules. Organic nitrogen compounds and nucleosides, nucleotides, and analogs were present in the purple and blue modules but not in the pink and light-cyan modules (Figure 4B). According to the pathway analysis, the module purple metabolites were mostly concentrated in retinol metabolism and propanoate metabolism (Figure 4G; Supplementary Table 20). Furthermore, the module pink metabolites were mostly concentrated in riboflavin metabolism, D-glutamate and D-Glutamine metabolism, and arginine biosynthesis (Figure 4H; Supplementary Table 21). Pathway analysis demonstrated that the module blue metabolites were mostly concentrated in alanine, aspartate and glutamate metabolism, and purine metabolism (Figure 4I; Supplementary Table 22). Pathway analysis revealed that the module light-cyan metabolites were mostly concentrated in ascorbate and aldarate metabolism and valine, leucine, and isoleucine biosynthesis (Figure 4J; Supplementary Table 23).

3.6. Analysis of unspecified proteomics and metabolomics data

To establish comprehensive profiling of AS at different stages and to determine the interactions between proteins and their metabolites, a multi-omics study incorporating proteomic and nonspecific metabolic data from the same biological samples was conducted. According to the DIABLO model, the unspecified metabolomic data and proteomic data of patients with different stages of AS were considerably different. The strong correlation between the latent components of the two omics datasets indicates that the DIABLO models of the two datasets are in full conformity. Proteins and metabolites were found to have a robust positive and negative correlation (Supplementary Figures 9-11). Identifying four key groups of coregulated characteristics to the underlying elements of the multi-omics dataset, which may be indicative of different stages of AS. Analysis of functional enrichment indicated that proteins between AIT and HC groups of the coregulated features were mostly enriched in the regulation of mitochondria, such as aerobic respiration, mitochondrial outer membrane, tricarboxylic acid cycle (TCA) enzyme complex, and energy derivation by oxidation of organic compounds (Figure 5A). Metabolites between AIT and HC groups of the coregulated features were mostly enriched in glutamate, aspartate, and alanine metabolism (Figure 5B; Supplementary Tables 24-26). Analysis of functional enrichment indicated that proteins between APNL and AIT groups of the coregulated features were mostly enriched in endocytosis (e.g., endocytic vesicle membrane, phagocytic vesicle) and exocytosis (e.g., secretory granule lumen) (Figure 5C; Supplementary Tables 27 and 28). Metabolites between APNL and AIT groups of the coregulated features were not significantly enriched in any pathway. Analysis of functional enrichment indicated that proteins between APL and APNL groups of the coregulated features were mostly enriched in the regulation of inflammation (e.g., negative regulation of hydrolase activity) and extracellular matrix (e.g., hyaluronan metabolic process) (Figure 5D). Metabolites between APL and APNL groups of the coregulated features were mostly enriched in amino acid metabolism (e.g., arginine biosynthesis, D-Glutamine, and D-glutamate metabolism) (Figure 5E; Supplementary Tables 29-31). Analysis of functional enrichment indicated that proteins between AP and AIT groups of the coregulated features were mostly enriched in ribosomes (e.g., ribosomal subunit, cytosolic ribosome) (Figure 5F; Supplementary Tables 32 and 33). Furthermore, metabolites between AP and AIT groups of the coregulated features were not significantly enriched in any pathway.

ISSN: 2688-8653

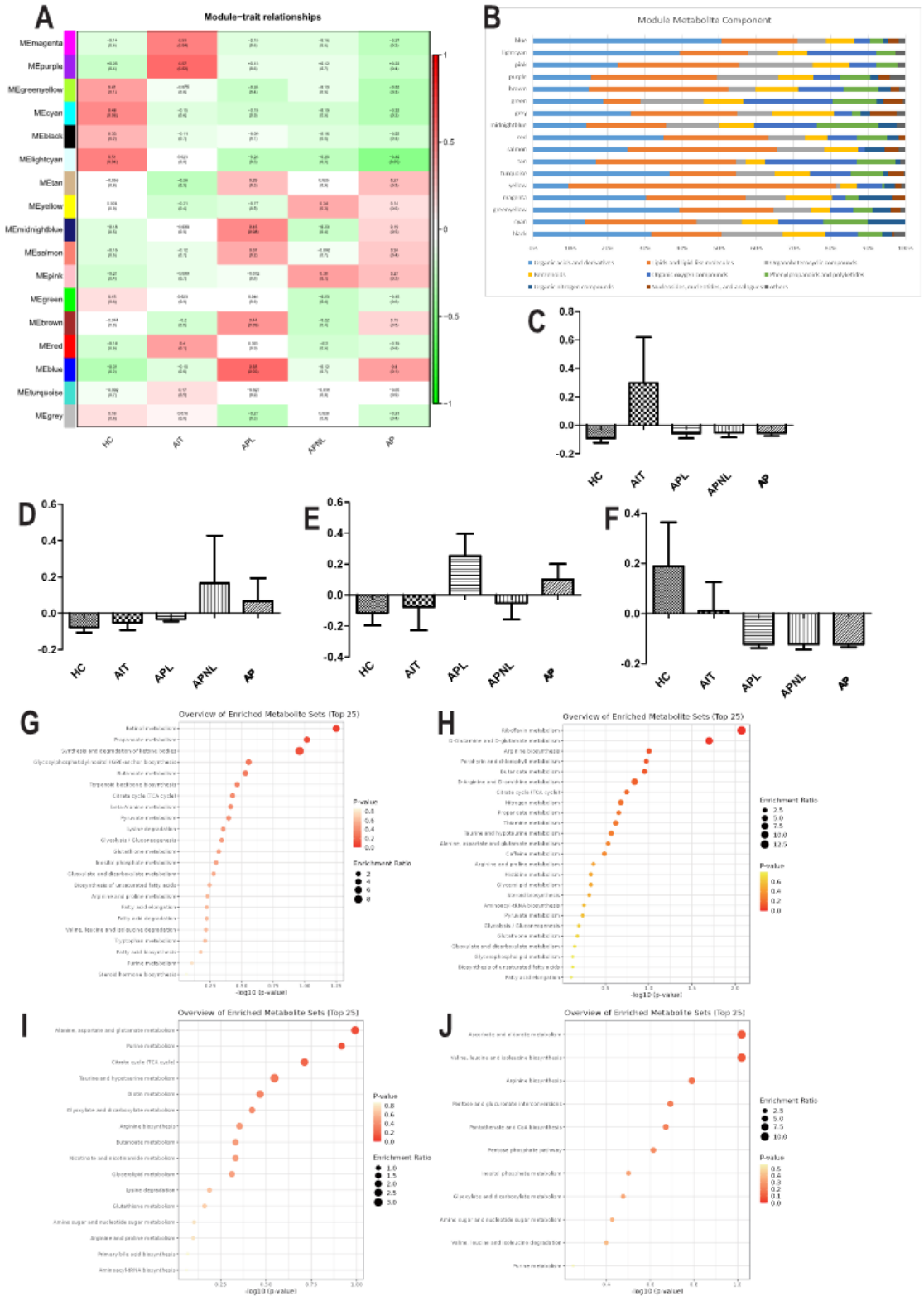

Figure 4: (A) Heatmap representation of the correlation between module eigenmetabolites and different phenotypes. (B) The distribution of metabolite members in each module. (C) Synthetic eigenmetabolite analysis of the module purple, which is highly correlated with AIT. (D) Synthetic eigenmetabolite analysis of the module pink, which is highly correlated with APNL. (E) Synthetic eigenmetabolite analysis of the module blue, which is highly correlated with APL. (F) Synthetic eigenmetabolite analysis of the module light-cyan, which is highly correlated with AP.

ISSN: 2688-8653

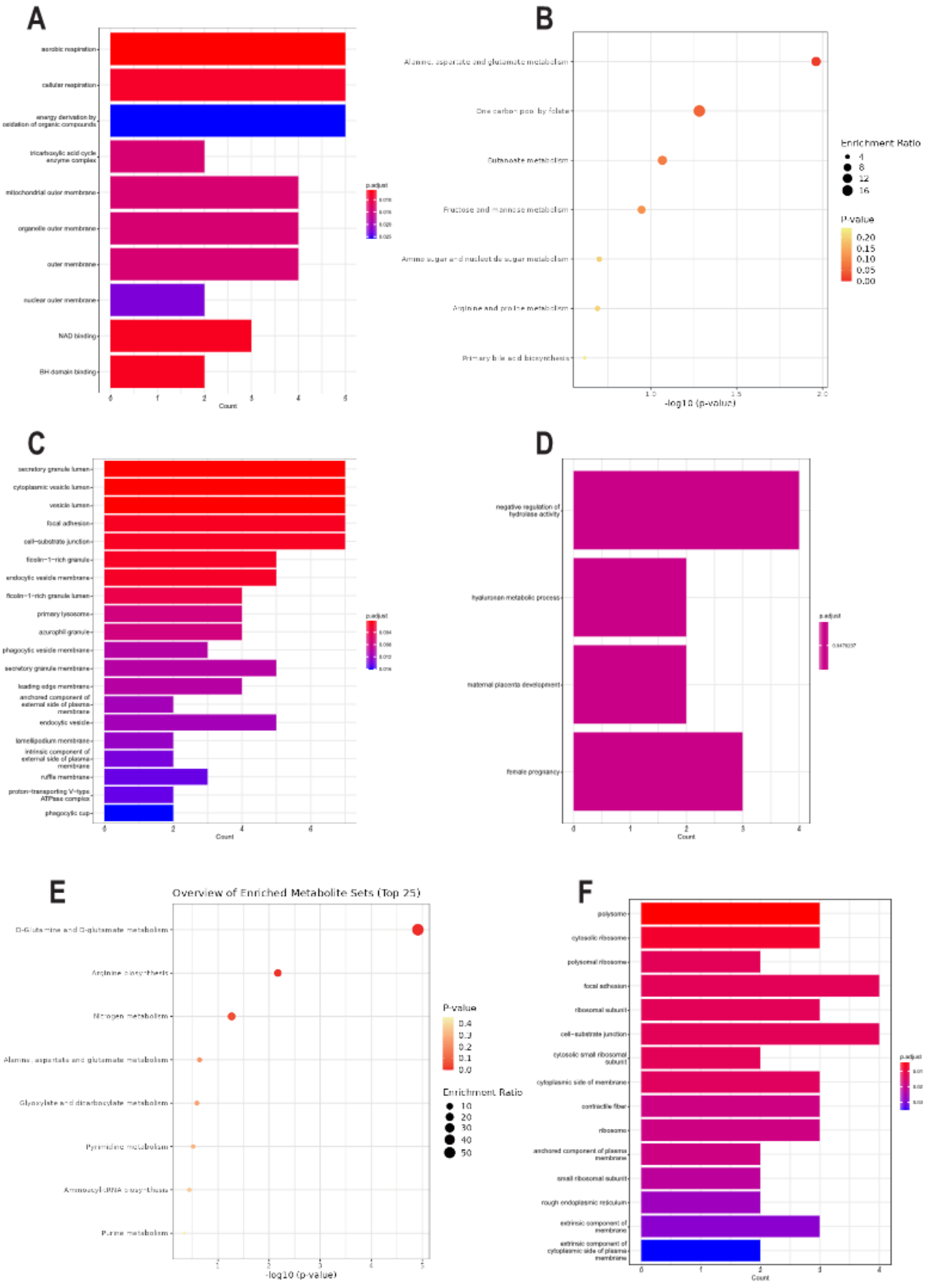

Figure 5: (A) GO terms enriched by the key proteins in AIT. (B) KEGG pathways enriched by the key metabolites in AIT. (C) GO terms enriched by the key proteins in APNL. (D) GO terms enriched by the key proteins in APL. (E) KEGG pathways enriched by the key metabolites in APL. (F) GO terms enriched by the key proteins in AP.

ISSN: 2688-8653

3.7. Melatonin–putative target network

After taking out duplicates from the PharmMapper, TargetNet, DrugBank, SwissTargetPrediction, and TCMSP databases, a total of 156 melatonin targets were found (Supplementary 1; Supplementary Table 36). Using Cytoscape 3.9.1, the melatonin-target network was then established. There were 17 known targets, representing 10.9% of the total targets, and 145 putative targets, representing 92.9% of the total targets. In addition, six crossing targets existed between the putative and known targets (Supplementary Figure 12).

3.8. PPI network of AS targets

From the NCBI, GeneCards, and DisGeNET databases, a total of 392 AS-related targets were extracted. To illustrate the interaction of AS-related targets, a PPI network was created (Supplementary Figure 12; Supplementary Tables 34 and 35). The mean values for degree centrality (DC), betweenness centrality (BC), and closeness centrality (CC) were 13.3617, 538.4965, and 105.8021, which were used to find 54 relevant AS-related targets.

3.9. PPI network of the potential therapeutic targets

Using the Venn Diagram (http://bioinformatics.psb.ugent.be/webtools/Venn/), twenty shared melatonin and AS targets (possible therapeutic targets) were identified. Then, a PPI network comprised of these 20 common targets was built (Supplementary Figure 13; Supplementary Table 37). To identify the hub targets in this intricate biological network, the topological parameters were investigated. Based on the mean values of BC, CC, and DC, this PPI network has five hub targets, including ALB, AKT1, PTGS2, PPARG, and NCOA2. Meanwhile, each of the five hub targets was a key AS-related target (Supplementary Table 38).

3.10. GO enrichment analysis

The 20 potential targets were investigated via R-version 4.1.3 clusterProfiler. The metabolic process of ROS, muscle cell proliferation, tube size, tube diameter, and blood vessel diameter regulation were the top five enriched biological processes (BP) of melatonin against AS effects. AKT1, PTGS2, and PPARG, three of the five hub targets, were also enriched in the top five BPs (Supplementary Figure 13).

3.11. KEGG enrichment analysis of the potential targets:

Using R-version 4.1.3 clusterProfiler, the KEGG enrichment analysis was performed on 20 therapeutic targets and provided 22 pathways. After sorting the genes enriched in each pathway, a melatonin-target-pathway network was built. Lipid and atherosclerosis (hsa05417) were significantly enriched. Using the community cluster (Glay) technique of clustermaker2, the target-pathway network was split into 5 functional modules to fully comprehend the mechanism by which melatonin treats AS (Supplementary Figure 14). Module 1 included four pathways, including the Longevity regulating pathway (hsa04211), Lipid and atherosclerosis (hsa05417), FoxO signaling pathway (hsa04068), and Neutrophil extracellular trap formation (hsa04613). Module 2 included four pathways, including the Endocrine resistance (hsa01522), Thyroid hormone signaling cascade (hsa04919), Estrogen signaling cascade (hsa04915), and Prolactin signaling cascade (hsa04917). Furthermore, module 3 contained seven pathways, i.e., the Diabetic cardiomyopathy (hsa05415), VEGF signaling cascade (hsa04370), AS and fluid shear stress (hsa05418), Platelet activation (hsa04611), sphingolipid signaling cascade (hsa04071), diabetes associated AGE-RAGE signaling cascade (hsa04933), Coronavirus disease - COVID-19 (hsa05171), and Relaxin signaling cascade (hsa04926). Module 4 comprised three pathways, including the TNF signaling pathway (hsa04668), C-type lectin receptor signaling pathway (hsa04625), and IL-17 signaling pathway (hsa04657). Module 5 comprised three pathways, including the Non-alcoholic fatty liver disease (hsa04932), AMPK signaling pathway (hsa04152), and Osteoclast differentiation (hsa04380). Furthermore, each of the 22 pathways

ISSN: 2688-8653

in the KEGG database also has its pathway class recorded. Simultaneously, five sub-networks were constructed in accordance with the pathway class to thoroughly explain the multi-mechanism effect of melatonin on AS (Supplementary Figure 15; Supplementary Table 39).

3.12. Network pharmacology analysis together with metabolomics

Here in this study, an interaction network was built on the basis of network pharmacology and metabolomics to provide a complete overview of how melatonin works against AS. To gather the compound-reaction-enzyme-gene networks, several metabolites were integrated into Cytoscape's MetScape plugin. Moreover, three key targets, including NOS3, PLA2G10, and MPO, were identified by comparing the possible targets discovered in network pharmacology with the genes in the MetScape study. The associated significant metabolites were phosphatidylcholine, glycine, L-Serine, phosphoenolpyruvate, L-Tryptophan, L-Methionine, L-Phenylalanine, L-Arginine, L-Tyrosine, IDP, uracil, myo-Inositol, (S)-Malate, Nicotinamide, L-Threonine, 3-Phospho-D-glycerate, guanine, D-Glycerate, hypoxanthine, 3,4-Dihydroxy-L-phenylalanine, 5-Oxoproline, N-(L-Arginino)succinate, 5-Guanidino-2-oxopentanoate, L-Allothreonine and N-(omega)-Hydroxyarginine. The affected pathways were biopterin metabolism, glycerophospholipid metabolism, bile acid biosynthesis, glycine, threonine serine, and alanine metabolism, glycosphingolipid metabolism, glycolysis and gluconeogenesis, leukotriene metabolism, methionine, and cysteine metabolism, lysine metabolism, phosphatidylinositol phosphate metabolism, pyrimidine metabolism, purine metabolism, porphyrin metabolism, tyrosine metabolism, tryptophan metabolism, TCA cycle, urea cycle and metabolism of proline, glutamate, arginine, asparagine, and aspartate, vitamin B3 (nicotinate and nicotinamide) metabolism, vitamin B9 (folate) metabolism, arachidonic acid metabolism, and linoleate metabolism. (Supplementary Figures 16 and 17) They may play essential roles in the therapeutic effect of melatonin on AS. The most important ones were the urea cycle and the metabolism of tyrosine, proline, arginine, glutamate, asparagine, and aspartate.

3.13. Molecular docking

Three key targets were chosen for the docking study with melatonin. Each target's active site characteristics were computed. The poorer docking affinity represents the higher interacting capacity between melatonin and its targets, and the binding posture with the highest affinity was chosen to investigate the interaction between melatonin and its targets. Except for NOS3, the interacting affinity between the remaining targets and melatonin was below -5 kcal/mol, suggesting a significant interacting affinity (Figure 6D). Melatonin may ameliorate AS by modulating the activity of these proteins. Figure 6 depicts the mechanism of melatonin interacting with the key targets. Using Figure 6A as an illustration, melatonin arrived at the active site of MPO and formed hydrogen bonds with residues VAL-217, GLY-212, and ARG-592.

ISSN: 2688-8653

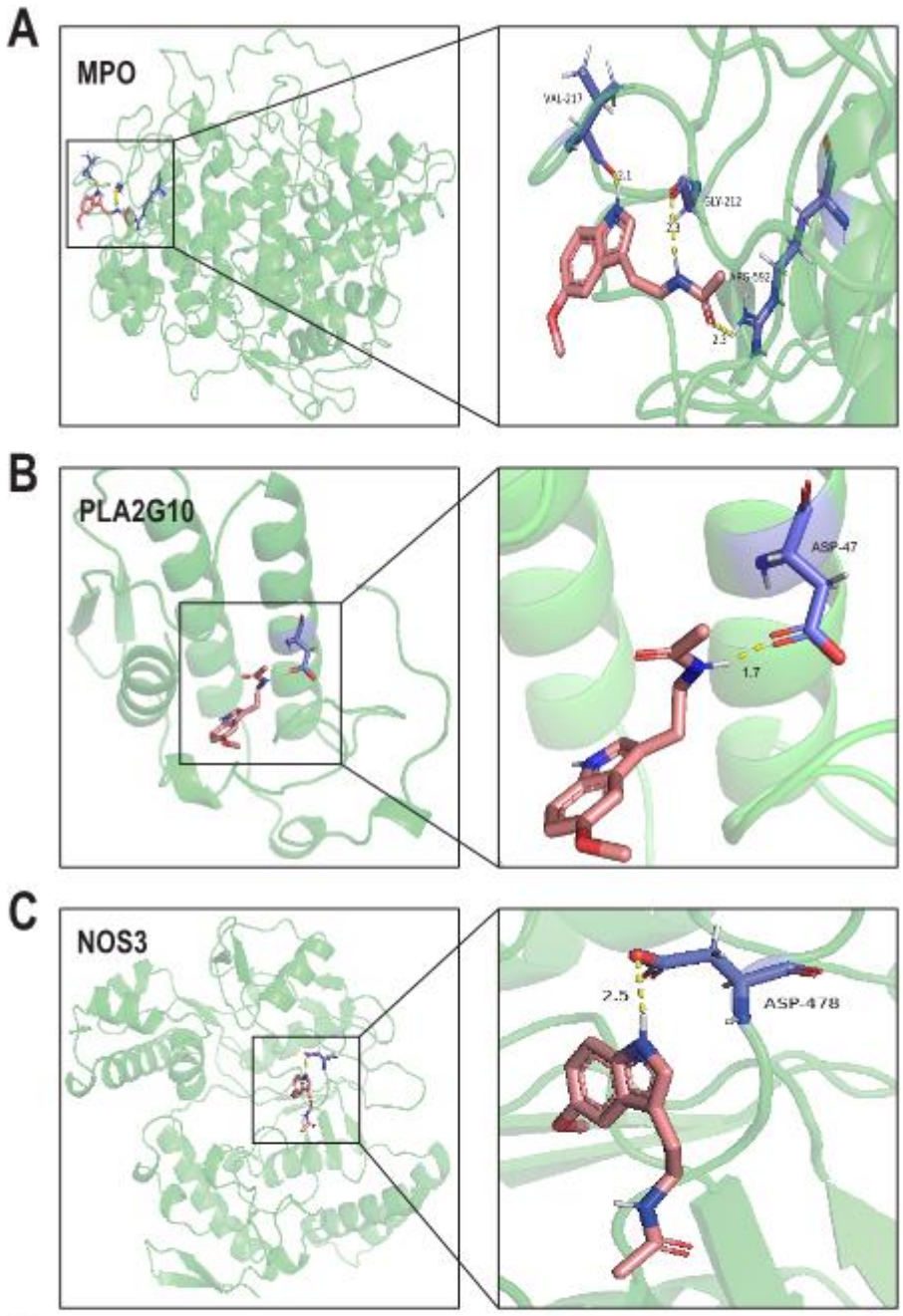

D

Related pathway	Key target	Affinity/(kcal/mol)
Tyrosine metabolism	MPO	-8.0
Arachidonic acid metabolism	PLA2G10	-7.0
Urea cycle and metabolism of arginine, proline, glutamate, aspartate and asparagine	NOS3	-3.8

Figure 6: (A) The 3D interaction diagrams of melatonin and MPO. (B) The 3D interaction diagrams of melatonin and PLA2G10. (C) The 3D interaction diagrams of melatonin and NOS3. (D) The information of key targets, pathways, and docking results.

4. Discussion

Atherosclerotic cardiovascular disease is becoming the leading cause of death globally [40]. Clarifying the pathophysiological features of AS and the specific mechanism of melatonin

ISSN: 2688-8653

against AS might aid in reducing its morbidity and mortality. In this research, we investigated 19 iliac artery samples by proteomics and metabonomics to reveal the change of proteins and metabolites in different stages of AS. To establish a reliable network for system biology study from proteins to the final metabolic product, a combined multi-omics analysis of proteomics and metabolomics data was carried out using the same biological materials. Moreover, metabolomics and network pharmacology were combined to elucidate the underlying mechanism of melatonin against AS.

Following differential expression analysis, 96 DEPs and 31 DEMs were identified between AIT and HC groups. Analyses of functional enrichment of these DEPs revealed that GO terms of inflammation and lipid regulation processes (e.g., fatty-acyl-CoA binding) were significantly enriched. The evaluation of these DEMs' metabolic pathways revealed that the ketone body, ascorbate, aldarate, and purine metabolic pathways were considerably enriched. The metabolism of ketone bodies was abnormal in AS [41]. Fatty-acyl-CoA was found associated with AS [42]. This suggests ketone bodies' metabolism and regulation of fatty-acyl-CoA may have been disrupted in the subclinical AS stage. In WGCNA analysis, functional enrichment analysis of proteins in the tan module showed that the GO terms of vesicle lumen and oxidative stress were significantly enriched. Pathways analysis of metabolites in the purple module showed that retinol metabolism was significantly enriched. Vesicle lumen-like exosomes play an important role in AS progress [43]. This suggests regulation of the vesicle lumen may have been disrupted in the subclinical atherosclerotic stage. Through integrated multi-omics analysis, thirty proteins were identified as possible biomarkers of AIT. Functional enrichment analysis of these proteins showed AIT was mainly associated with mitochondria dysfunction. Results indicated that proteins' metabolites were primarily involved in glutamate, aspartate, and alanine metabolism. These findings suggested a possible regulatory interaction between mitochondrial dysfunction and amino acid metabolism, which might offer a feasible strategy for inhibiting the progression of AIT.

The differential expression analysis detected 38 DEPs and 52 DEMs between the APL and APNL groups. Analyses of the functional enrichment of these DEPs showed that there was a significant level of enrichment in the extracellular matrix and inflammatory processes. Pathways analysis of these DEMs showed that amino acid (e.g., glycine, phenylalanine, tyrosine, tryptophan, and cysteine) metabolism were significantly enriched. Metabolic factors have a direct influence on regulating the activity of immune cells. The inflammation-induced metabolism of aromatic amino acids, namely tryptophan and phenylalanine, thus plays a major role [44]. Immune activation and inflammation are associated with increased phenylalanine/tyrosine ratios in cardiovascular disease patients [45]. These results indicated phenylalanine, tyrosine, and tryptophan biosynthesis may play an important role in AS progression, which might be a useful strategy for preventing the progress of AS. Through integrated multi-omics analysis, 15 proteins were identified as possible biomarkers of APL. A functional enrichment study of these proteins revealed that APL is mainly correlated to inflammation and extracellular matrix. Results indicated that proteins' metabolites were mainly involved in amino acid metabolism, including D-glutamate and arginine metabolism. These findings suggest a possible regulatory interaction between inflammation, extracellular matrix, and amino acid metabolism. which may serve as a candidate strategy for preventing the progress of AS.

In accordance with differential expression analysis, 123 DEPs and 17 DEMs were identified between AP and AIT groups. Analyses of functional enrichment of these DEPs revealed that GO terms of oxidative stress, proteasome, and endopeptidase were significantly enriched. Pathways analysis of these DEMs showed that purine metabolism and pentose phosphate pathway was significantly enriched. The second messengers cAMP and cGMP have been found to have a negative effect on a number of immune cell responses [46]. In our study, purine nucleotide metabolism was found significantly enriched in the APNL stage and purine

ISSN: 2688-8653

metabolism was found significantly enriched in AIT, APL, and AP stages. This suggests purine nucleotide metabolism may be disrupted in the AIT stage and has been disrupted in the APNL stage.

Ultimately, by integrating metabolomics with network pharmacology, this integrated technique identifies 3 key targets (PLA2G10, MPO, and NOS3) and 3 key pathways (metabolism of arginine, glutamate, proline, aspartate and asparagine, urea cycle, Arachidonic acid metabolism, and tyrosine metabolism) (Figure 7) and gives a more accurate network of melatonin against the different stages of AS. Arachidonic acid (AA) metabolism represents a potential therapeutic pathway in AS [47]. The release of AA from phospholipids in the cell membrane accounts for the majority of endogenous AA synthesis. This activity is carried out by the phospholipase A2 (PLA2) subfamily and is triggered by several cell-activating signals, including activation of the purinergic receptor and toll-like receptor 4 (TLR4) [48]. Here in this study, purine nucleotide metabolism was found significantly enriched in the APNL stage and purine metabolism was found significantly enriched in AIT, APL, and AP stages. This may provide a new understanding of the mechanism by which melatonin inhibits AS progression. AA metabolites are associated with chemotaxis, inflammation, and efferocytosis. The metabolism of AA and cholesterol are connected [47]. According to the current analysis, melatonin can regulate arachidonic acid metabolism by acting on PLA2G10, thereby inhibiting the progression of AIT to APNL.

MPO, also known as myeloperoxidase, is associated with increased cardiovascular events [49]. MPO exerts its oxidative potential in atherosclerotic lesions by using several co-substrates with H2O2 to create reactive intermediates [50]. MPO has been related to lesion rupture, superficial erosion, and endothelium apoptosis in plaques [51]. Additionally, nitrite, a byproduct of the metabolism of NO radicals, may be converted by MPO into a NO radical. This can start lipid peroxidation and lead to the production of nitrotyrosine and/or nitrated lipids [52]. Based on the obtained results, melatonin can regulate tyrosine metabolism by acting on MPO, thereby inhibiting the progression of atherosclerotic plaques.

An early indicator of AS is endothelial dysfunction, which can be identified before structural variations to the vessel wall are detectable on ultrasound or angiography [53]. Endothelial dysfunction is mostly attributed to changes in nitric oxide (NO) bioavailability, NO signaling, and ROS levels. Furthermore, NO is generated in the endothelium by NOS3 (endothelial NOS), which utilizes l-arginine as a substrate. Arginase, a key urea cycle enzyme, also uses l-arginine. It therefore directly competes with NOS3 for their shared substrate l-arginine and restricts NOS3's access to it, reducing NO synthesis and boosting ROS generation through NOS uncoupling [54]. According to the current study, melatonin can slow the growth of atherosclerotic plaques by regulating the urea cycle and the metabolism of aspartate, glutamate, asparagine, arginine, and proline through NOS3.

ISSN: 2688-8653

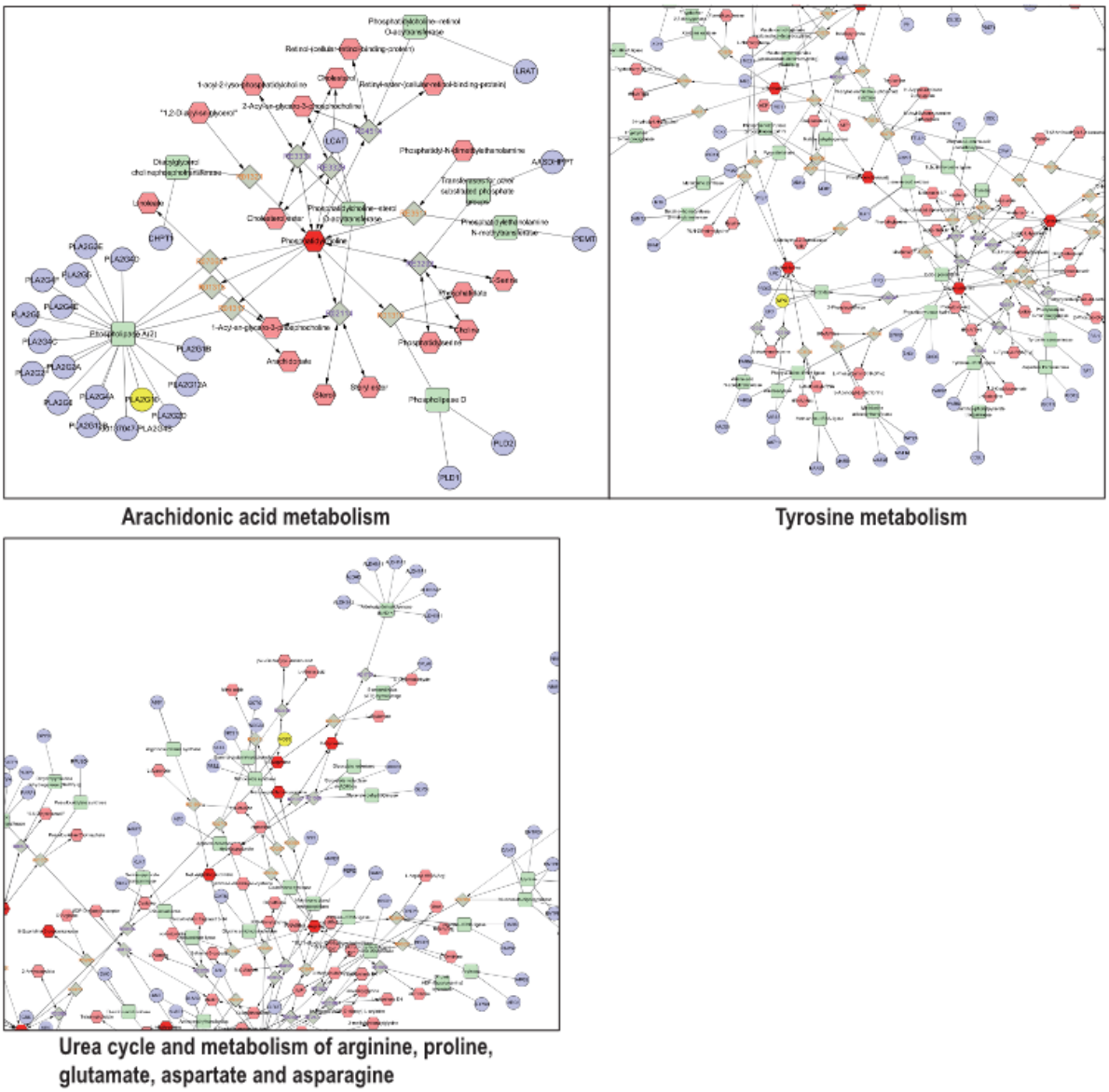

Figure 7: The compound-reaction-enzyme-gene networks of the key metabolites and targets. The red hexagons, grey diamonds, green round rectangles, purple circles, and yellow circles represent the active compounds, reactions, proteins, genes, and key genes, respectively.

5. Conclusion

Taken together, this study provides an integrated metabolomics analysis and proteomic information collected from matching biological samples taken from healthy individuals (control group) and AS patients at various phases. The discovered distinctive proteins and metabolites constructed a complicated network to illustrate the key connections between the various phases of AS. Purine nucleotides metabolism was found to be related to atherosclerotic plaque without lipid core stage and purine metabolism was found to be related to subclinical atherosclerotic stage and atherosclerotic plaque with lipid core stage, indicating purine nucleotide metabolism may be disrupted in arterial intima thickening stage and has been disrupted in atherosclerotic plaque without lipid core stage. Herein, several amino acids, such as alanine, aspartate, glutamate, and arginine, were found to be associated with different stages of atherosclerosis. These altered metabolites may be beneficial for diagnosing and treating the

ISSN: 2688-8653

various phases of AS. According to the network pharmacology and metabolomics study, a unique integrated technique was first established to investigate the underlying mechanisms and principle targets of melatonin in treating various phases of AS. The combined study indicated three key targets (NOS3, PLA2G10, and MPO), in addition to the corresponding metabolites and pathways. Molecular docking further verified these targets. This study lays the groundwork for future therapeutic use by giving both empirical evidence and theoretical support for a more in-depth analysis of mechanisms. Additional comprehensive molecular biology tests are required to confirm the precise pathways. It also offers a new paradigm for identifying the principal mechanisms of the pharmacological effects of drugs on different stages of the disease.

Acknowledgements

The authors would like to thank all the reviewers who participated in the review and MJEditor (www.mjeditor.com) for its linguistic assistance during the preparation of this manuscript.

National Natural Science Foundation of China (No. 81870848, 82171410), Fundamental Research Funds of Chinese Academy of Medical Sciences(No. 2019-RC-HL-026), and Shandong University Multidisciplinary Research and Innovation Team of Young Scholars(No. 2020QNQT019).

List of Abbreviations

AS: Atherosclerosis
WGCNA: Weighted gene coexpression network analysis
HC: health control
FASP: filter-aided sample preparation
UHPLC: ultra-high-pressure liquid chromatography
HILIC: hydrophilic interaction liquid chromatography
ESI: electrospray ionization
ISVF: IonSpray Voltage Floating
Gas1: Ion Source Gas1
Gas2: Ion Source Gas2
CUR: curtain gas
CCA: sparse canonical correlation analysis
SMILES: simplified molecular input line entry specification
OPLS-DA: Orthogonal partial least-squares discriminant analysis
FC: fold change
DEPs: differentially expressed proteins
VIP: variable importance in the projection
DEMs: differentially expressed metabolites
AIT: arterial intima thickening
APNL: atherosclerotic plaque without lipid core
APL: atherosclerotic plaque with lipid core
AP: atherosclerotic plaque
GO: gene ontology
IFN: interferon
Gβγ: G-protein beta-gamma

ISSN: 2688-8653

QC: Quality control
TCA: tricarboxylic acid cycle
DC: degree centrality
BC: betweenness centrality
CC: closeness centrality
BP: biological processes
AA: Arachidonic acid
PLA2: phospholipase A2
TLR4: toll-like receptor 4
NO: nitric oxide
NOS3: endothelial NOS

References

[1] D. Wolf and K. Ley: Immunity and inflammation in atherosclerosis, Circulation Research, Vol. 124 (2019) No. 2, p. 315-327.

[2] J.M. Tarkin, M.R. Dweck, N.R. Evans, et al.: Imaging atherosclerosis, Circulation Research, Vol. 118 (2016) No. 4, p. 750-769.

[3] S.S. Singh, C.S. Pilkerton, C.D. Shrader, et al.: Subclinical atherosclerosis, cardiovascular health, and disease risk: is there a case for the Cardiovascular Health Index in the primary prevention population?, BMC Public Health, Vol. 18 (2018) No. 1, p.429.

[4] V.G. de Yébenes, A.M. Briones, I. Martos-Folgado, et al.: Aging-associated miR-217 aggravates atherosclerosis and promotes cardiovascular dysfunction, Arteriosclerosis, Thrombosis, and Vascular Biology, Vol. 40 (2020) No. 10, p. 2408-2424.

[5] I.E. Hoefer, S. Steffens, M. Ala-Korpela, et al.: Novel methodologies for biomarker discovery in atherosclerosis, European Heart Journal, Vol. 36 (2015) No. 39, p. 2635-2642.

[6] Q. Chen, X. Liang, T. Wu, et al.: Integrative analysis of metabolomics and proteomics reveals amino acid metabolism disorder in sepsis, Journal of Translational Medicine, Vol. 20 (2022) No. 1, p. 123.

[7] N. Ruparelia, R. Choudhury: Inflammation and atherosclerosis: what is on the horizon?, Heart, Vol. 106 (2020) No. 1, p. 80-85.

[8] R.J. Reiter, D.X. Tan, S. Rosales-Corral, et al.: Mitochondria: central organelles for melatonin's antioxidant and anti-aging actions, Molecules, Vol. 23 (2018) No. 2, p. 509.

[9] Q. Ma, R.J. Reiter, Y. Chen, Role of melatonin in controlling angiogenesis under physiological and pathological conditions, Angiogenesis, Vol. 23 (2020) No. 2, p. 91-104.

[10] X. Wang, Y. Bian, R. Zhang, et al.: Melatonin alleviates cigarette smoke-induced endothelial cell pyroptosis through inhibiting ROS/NLRP3 axis, Biochemical and Biophysical Research Communications, Vol. 519 (2019) No. 2, p. 402-408.

[11] B. Ma, Y. Chen, X. Wang, et al.: Cigarette smoke exposure impairs lipid metabolism by decreasing low-density lipoprotein receptor expression in hepatocytes. Lipids in Health and Disease, Vol. 19 (2020) No. 1, p. 88.

[12] Y.T. Tung, P.C. Chiang, Y.L. Chen, et al.: Effects of melatonin on lipid metabolism and circulating irisin in sprague-dawley rats with diet-induced obesity, Molecules, Vol. 25 (2020) No. 15, p. 3329.

[13] K. Lu, X. Liu, W. Guo, Melatonin attenuates inflammation-related venous endothelial cells apoptosis through modulating the MST1-MIEF1 pathway, Journal of Cellular Physiology, Vol. 234 (2019) No. 12, p. 23675-23684.

[14] J.A. Boga, B. Caballero, Y. Potes, et al.: Therapeutic potential of melatonin related to its role as an autophagy regulator: A review, Journal of Pineal Research, Vol. 66 (2019) No. 1, p. e12534.

[15] N. Sadanandan, B. Cozene, J. Cho, et al.: Melatonin- A potent therapeutic for stroke and stroke-related dementia, Antioxidants, Vol. 9 (2020) No. 8, p. 672.

ISSN: 2688-8653

[16] F. Nduhirabandi, G.J. Maarman: Melatonin in heart failure: A promising therapeutic strategy?, Molecules, Vol. 23 (2018) No. 7, p. 1819.

[17] G. Tekin, S. İsbir, G. Şener, et al.: The preventive and curative effects of melatonin against abdominal aortic aneurysm in rats, Journal of Vascular Surgery, Vol. 67 (2018) No. 5, p. 1546-1555.

[18] Y. Zhang, X. Liu, X. Bai, et al.: Melatonin prevents endothelial cell pyroptosis via regulation of long noncoding RNA MEG3/miR-223/NLRP3 axis, Journal of Pineal Research, Vol. 64 (2018) No. 2, p. e12449.

[19] C. Karaaslan, S. Suzen, Antioxidant properties of melatonin and its potential action in diseases, Current Topics in Medicinal Chemistry, Vol. 15 (2015) No. 9, p. 894-903.

[20] D.L. Ren, A.A. Sun, Y.J. Li, et al.: Exogenous melatonin inhibits neutrophil migration through suppression of ERK activation, Journal of Endocrinology, Vol. 227, (2015) No. 1, p. 49-60.

[21] Z. Zhao, X. Wang, R. Zhang, et al.: Melatonin attenuates smoking-induced atherosclerosis by activating the Nrf2 pathway via NLRP3 inflammasomes in endothelial cells, Aging (Albany NY), Vol. 13 (2021) No. 8, p. 11363-11380.

[22] D. Leger, M.A. Quera-Salva, M.F. Vecchierini, et al.: Safety profile of tasimelteon, a melatonin MT1 and MT2 receptor agonist: pooled safety analyses from six clinical studies, Expert Opinion on Drug Safety, Vol. 14 (2015) No. 11, p. 1673-1685.

[23] T. Li, W. Zhang, E. Hu, et al.: Integrated metabolomics and network pharmacology to reveal the mechanisms of hydroxysafflor yellow A against acute traumatic brain injury, Computational and Structural Biotechnology Journal, Vol. 19 (2021) p. 1002-1013.

[24] D. Burtenshaw, M. Kitching, E.M. Redmond, et al.: Reactive oxygen species (ROS), intimal thickening, and subclinical atherosclerotic disease, Frontiers in Cardiovascular Medicine, Vol. 6 (2019) p. 89.

[25] M.A. Creager, M. Belkin, E.I. Bluth, et al.: 2012 ACCF/AHA/ACR/SCAI/SIR/STS/SVM/SVN/SVS Key data elements and definitions for peripheral atherosclerotic vascular disease: a report of the American College of Cardiology Foundation/American Heart Association Task Force on Clinical Data Standards (Writing Committee to develop Clinical Data Standards for peripheral atherosclerotic vascular disease), Journal of the American College of Cardiology, Vol. 59 (2012) No. 3, p. 294-357. Erratum in: Journal of the American College of Cardiology, Vol. 59 (2012) No. 7, p. 702. Erratum in: Journal of the American College of Cardiology, Vol. 62 (2013) No. 11, p. 1042.

[26] Z. Gu, L. Li, S. Tang, et al.: Metabolomics reveals that crossbred dairy buffaloes are more thermotolerant than Holstein cows under chronic heat stress, Journal of Agricultural and Food Chemistry, Vol. 66 (2018) No. 49, p. 12889-12897.

[27] G. Yu, L.G. Wang, Y. Han, et al.: clusterProfiler: an R package for comparing biological themes among gene clusters, OMICS, Vol. 16 (2012) No. 5, p. 284-287.

[28] A. Singh, C.P. Shannon, B. Gautier, et al.: DIABLO: an integrative approach for identifying key molecular drivers from multi-omics assays, Bioinformatics, Vol. 35 (2019) No. 17, p. 3055-3062.

[29] F. Rohart, B. Gautier, A. Singh, et al.: mixOmics: An R package for 'omics feature selection and multiple data integration, PLoS Computational Biology, Vol. 13 (2017) No. 11, e1005752.

[30] S. Kim, P.A. Thiessen, E.E. Bolton, et al.: PubChem substance and compound databases, Nucleic Acids Research, Vol. 44 (2016) No. D1, p. D1202-D1213.

[31] X. Wang, Y. Shen, S. Wang, et al.: PharmMapper 2017 update: a web server for potential drug target identification with a comprehensive target pharmacophore database, Nucleic Acids Research, Vol. 45 (2017) No. W1, p. W356-W360.

[32] A. Daina, O. Michielin, V. Zoete, SwissTargetPrediction: updated data and new features for efficient prediction of protein targets of small molecules, Nucleic Acids Research, Vol. 47 (2019) No. W1, p. W357-W364.

[33] Z.J. Yao, J. Dong, Y.J. Che, et al.: TargetNet: a web service for predicting potential drug-target interaction profiling via multi-target SAR models, Journal of Computer-Aided Molecular Design, Vol. 30 (2016) No. 5, p. 413-424.

[34] D.S. Wishart, Y.D. Feunang, A.C. Guo, et al.: DrugBank 5.0: a major update to the DrugBank database for 2018, Nucleic Acids Research, Vol. 46 (2018) No. D1, p. D1074-D1082.

ISSN: 2688-8653

[35] J. Ru, P. Li, J. Wang, et al.: TCMSP: a database of systems pharmacology for drug discovery from herbal medicines, Journal of Cheminformatics, Vol. 6 (2014) p. 13.

[36] D. Szklarczyk, A.L. Gable, D. Lyon, et al.: STRING v11: protein-protein association networks with increased coverage, supporting functional discovery in genome-wide experimental datasets, Nucleic Acids Research, Vol. 47 (2019) No. D1, p. D607-D613.

[37] D. Otasek, J.H. Morris, J. Bouças, et al.: Cytoscape Automation: empowering workflow-based network analysis, Genome Biology, Vol. 20 (2019) No. 1, p. 185.

[38] G.M. Morris, R. Huey, W. Lindstrom, et al.: AutoDock4 and AutoDockTools4: Automated docking with selective receptor flexibility, Journal of Computational Chemistry, Vol. 30 (2009) No. 16, p. 2785-2791.

[39] O. Trott, and A.J. Olson: AutoDock Vina: improving the speed and accuracy of docking with a new scoring function, efficient optimization, and multithreading, Journal of Computational Chemistry, Vol. 31 (2010) No. 2, p. 455-461.

[40] P. Libby: The changing landscape of atherosclerosis, Nature, Vol. 592 (2021) No. 7855, p. 524-533.

[41] S. Nasser, V. Vialichka, M. Biesiekierska, et al.: Effects of ketogenic diet and ketone bodies on the cardiovascular system: Concentration matters, World Journal of Diabetes, Vol. 11 (2020) No. 12, p. 584-595.

[42] T.A. Bell III, M.D. Wilson, K. Kelley, et al.: Monounsaturated fatty acyl-coenzyme A is predictive of atherosclerosis in human apoB-100 transgenic, LDLr-/- mice, Journal of Lipid Research, Vol. 48 (2007) No. 5, p. 1122-1131.

[43] C. Wang, Z. Li, Y. Liu, et al.: Exosomes in atherosclerosis: performers, bystanders, biomarkers, and therapeutic targets, Theranostics, Vol. 11 (2021) No. 8, p. 3996-4010.

[44] B. Strasser, B. Sperner-Unterweger, D. Fuchs, et al.: Mechanisms of inflammation-associated depression: Immune influences on tryptophan and phenylalanine metabolisms, in: R. Dantzer, and L. Capuron (editors), Inflammation-Associated Depression: Evidence, Mechanisms and Implication, (Springer, Cham 2017), p. 95-115.

[45] Z. Guľašová, S.G. Guerreiro, R. Link, et al.: Tackling endothelium remodeling in cardiovascular disease, Journal of Cellular Biochemistry, Vol. 121 (2020) No. 2, p. 938-945.

[46] A.C. Newton, M.D. Bootman, J.D. Scott, Second messengers, Cold Spring Harbor Perspectives in Biology, Vol. 8 (2016) No. 8, p. a005926.

[47] T. Sonnweber, A. Pizzini, M. Nairz, et al.: Arachidonic acid metabolites in cardiovascular and metabolic diseases, International Journal of Molecular Sciences, Vol. 19 (2018) No. 11, p. 3285.

[48] V.S. Hanna, E.A.A. Hafez, Synopsis of arachidonic acid metabolism: A review, Journal of Advanced Research, Vol. 11 (2018) p. 23-32.

[49] G. Ndrepepa, Myeloperoxidase - A bridge linking inflammation and oxidative stress with cardiovascular disease, Clinica Chimica Acta, Vol. 493 (2019) p. 36-51.

[50] G. Marsche, J.T. Stadler, J. Kargl, et al.: Understanding myeloperoxidase-induced damage to HDL structure and function in the vessel wall: Implications for HDL-based therapies, Antioxidants, Vol. 11 (2022) No. 3, p. 556.

[51] O. Soehnlein, S. Steffens, A. Hidalgo, et al.: Neutrophils as protagonists and targets in chronic inflammation, Nature Reviews Immunology, Vol. 17 (2017) No. 4, p. 248-261.

[52] D.I. Pattison, M.J. Davies, C.L. Hawkins, Reactions and reactivity of myeloperoxidase-derived oxidants: differential biological effects of hypochlorous and hypothiocyanous acids, Free Radical Research, Vol. 46 (2012) No. 8, p. 975-995.

[53] S. Berenji Ardestani, I. Eftedal, M. Pedersen, et al.: Endothelial dysfunction in small arteries and early signs of atherosclerosis in ApoE knockout rats, Scientific Repports, Vol. 10 (2020) p. 15296.

[54] J. Steppan, D. Nyhan, D.E. Berkowitz: Development of novel arginase inhibitors for therapy of endothelial dysfunction, Frontiers in Immunology, Vol. 4 (2013) p. 278.